International Journal of Biological Macromolecules 168 (2021) 350–355

Contents lists available at ScienceDirect

International Journal of Biological Macromolecules

journal homepage: http://www.elsevier.com/locate/ijbiomac

Colorado potato beetle alpha-amylase: Purification, action pattern and subsite mapping for exploration of active centre

Csaba Hámori [a], Judit Remenyik [b], Lili Kandra [a], Gyöngyi Gyémánt [a,*]

[a] Department of Inorganic and Analytical Chemistry, Faculty of Sciences and Technology, University of Debrecen, H-4032 Debrecen, Hungary
[b] Institute of Food Technology, Faculty of Agricultural and Food Sciences and Environmental Management, University of Debrecen, H-4032 Debrecen, Hungary

ARTICLE INFO

Article history:
Received 29 September 2020
Received in revised form 29 October 2020
Accepted 8 December 2020
Available online 11 December 2020

Keywords:
Insect α-amylase
Bond cleavage frequency
Subsite structure

ABSTRACT

Colorado potato beetle is an invasive insect herbivore and one of the most challenging agricultural pests globally. This study is the first characterization of the active centre of Colorado potato beetle (*Leptinotarsa decemlineata*) α-amylase (LdAmy). Bond cleavage frequency values for LdAmy were determined by HPLC product analysis on a chromophore labelled maltooligomer substrate series. Binding energies between amino acid moieties of subsites and glucose residues of substrate were calculated. Active site contains six subsites in the binding region of LdAmy; four glycone- (−4, −3, −2, −1) and two aglycone-binding sites (+1, +2). Subsite map calculation resulted in apparent binding energies −11.8 and − 11.0 kJ/mol for subsites (+2) and (−3), respectively, which revealed very favorable interactions at these positions. Structures of binding sites of LdAmy and mammalian α-amylases show similarity, but there are variations in the binding energies at subsite (−2) and (−4). Differences were interpreted by comparison of amino acid sequences of human salivary α-amylase (HSA) and porcine pancreatic α-amylase (PPA) and two insect (*Leptinotarsa decemlineata* and *Tenebrio molitor*) enzymes. The observed substitution of positively charged His305 in HSA at subsite (−2) with an acidic Asp in LdAmy in the same position may explain the obtained energy reduction.

1. Introduction

In insects, the digestion of starch depends only on amylases and α-glucosidases [1]. The sequences and some properties of α-amylases of different insect order origins (Diptera, Coleoptera, Heteroptera and Hymenoptera) have already been described [2–7], but mainly the cereal-eating insect α-amylases were studied [8,9]. The sole insect amylase with a known 3D structure is *Tenebrio molitor* larva α-amylase (TMA) (PDB: 1viw, 1clv, 1tmq, 1jae) [10] with a 50% sequence similarity to mammalian amylases like porcine pancreatic α-amylase (PPA) and human salivary α-amylase (HSA). α-Amylase enzymes (EC 3.2.1.1) belong to the GH13 family of glycoside hydrolyses according to a sequence-based classification [11], and they are characterized by a $(\beta/\alpha)_8$ barrel 3D structure with seven conserved regions. The active site of α-amylase family enzymes contains a strictly conserved triade of acidic groups as catalytic residues: a Glu as proton donor, an Asp as catalytic nucleophile, and an additional Asp involving in substrate binding [12]. The substrate binding region of α-amylases consists of a tandem array of subsites, where each subsite interacts with one glucose, the monomer unit of starch substrate, according to the subsite model [13]. The quantification of binding energies belonging to subsites is referred to as subsite mapping. Substrates bind productively if a susceptible bond lies over the catalytic site, and the bond is cleaved. *Endo*-carbohydrase enzymes, like α-amylases, can form more productive binding modes, and the relative rate of the formation of each product is called bond cleavage frequency (BCF). By using BCF data obtained for a substrate series, it is possible to calculate the subsite binding energy for every subsite in the enzyme binding region with the exception of the two subsites adjacent to the catalytic site, which are occupied in every productive complex [14,15]. Subsite maps were evaluated earlier in our research group for α-amylases of different origin such as PPA, HSA, *Bacillus licheniformis* (BLA), and two barley α-amylase isoenzymes [16–19].

There has been an increased focus on the research of insect amylases, and the properties of several insect amylases have been reported since 2000 [20–25] We have recently studied and published the process of carbohydrate digestion in the gut of Colorado potato beetle (CPB) [26]. *Leptinotarsa decemlineata* (Say) (Coleoptera: Chrysomelidae) is

Abbreviations: BCF, bond cleavage frequency; BLA, *Bacillus licheniformis* α-amylase; CNP, 2-chloro-4-nitrophenyl; CPB, Colorado potato beetle; GalG2CNP, 2-chloro-4-nitrophenyl 4-O-β-D-galactopyranosyl-α-maltoside; G_n, maltooligomer, where n is the number of glucose unit; HPLC-DAD, high performance liquid chromatography with diode array detector; HSA, human salivary α-amylase; LdAmy, *Leptinotarsa decemlineata* α-amylase; PPA, porcine pancreatic α-amylase; SUMA, SUbsite Mapping of Amylases software; TMA, *Tenebrio molitor* α-amylase.

* Corresponding author at: University of Debrecen, Department of Inorganic and Analytical Chemistry, P.O. Box 400, Egyetem tér 1., Debrecen H-4002, Hungary.
E-mail address: gyemant@science.unideb.hu (G. Gyémánt).

https://doi.org/10.1016/j.ijbiomac.2020.12.071

an invasive herbivore insect and one of the most challenging agricultural pests because it is able to adapt to a variety of solanaceous plants, a wide range of abiotic and biotic stresses, and variable climates. The annual costs of ongoing management reach tens of millions of dollars due to the global expansion of CPB and its ability to rapidly evolve resistance to insecticides. *L. decemlineata* genome was published in 2018, and C and N terminal parts of some GH13 proteins was recognized among the 182 GH enzymes, but α-amylase sequence was not identified [27]. The gene (Acc. LOC111504815) encoding an α-amylase like protein (Sequence ID: XP_023015287.1) was found in Gene database at NCBI (National Center for Biotechnology Information) using sequence of *Tenebrio molitor* α-amylase as a template.

Despite the studies on α-amylases of insect origin in general and in *L. decemlineata* in particular (reviewed above), there are a lack of data relating to the subsite structure of the α-amylase, which enzyme is active in the midgut of this insect. Considering the central role of α-amylase in the carbohydrate digestion of CPB, the mapping of the active site should provide a rational basis for the development of new inhibitor molecules with increased affinity for LdAmy [1–36].

Amylase inhibitors are found in the seeds of plants such as cereals and legumes, but new promising synthetic inhibitors are also constantly developed [28,29]. CPB α-amylase was purified from the extract of insect imago midgut using an effective affinity chromatographic step. Action pattern on a chromophore containing maltooligomer substrate series was determined by HPLC. Based on the obtained bond cleavage frequency (BCF) data, subsite map calculation was carried out with SUMA (SUbsite Mapping of Amylases) software developed by our research group [30]. SUMA uses the experimentally determined BCFs for the identification of the number of subsites, the position of the catalytic site and for calculation of subsite binding energies.

2. Materials and methods

2.1. Enzyme purification

The preparation of LdAmy was published earlier [26]. Briefly, the digestive tracts of *L. decemlineata* imagoes were removed from the beetles after their decapitation and cutting up their abdomen and thorax. The prepared digestive tract was put into 500 μL physiological saline solution (0.9% NaCl, pH 6.5), vortexed then centrifuged for 5 min on 10,000*g* at 5 °C. The supernatants were collected and stored at −80 °C until accomplishing activity measurements and further purification. Since α- and β-glucosidase were also present in the extract [26], α-amylase was purified from the contaminants by affinity chromatography on a cross-linked starch gel. We used the method developed by Kobayashi and his coworkers with some alterations [31]. The applied starch stationary phase was prepared using 2 g water soluble starch (Sigma-Aldrich, St. Louis, Missouri, USA), 1.2 mL 5 mM NaOH, 1.2 mL distilled water and 0.8 mL epichlorohydrin (Sigma-Aldrich, St. Louis, Missouri, USA). The reaction mixture was heated in a water bath at 90 °C for 10 min and incubated overnight. The solid product was crushed in a mortar and washed with distilled water three times. The pure starch gel was filled into a column, washed and equilibrated with 40 mM acetate buffer (pH 5.2) containing 1 M ammonium sulphate. The extract of beetle gut was added into the column. 1 mL of fractions were collected, and the concentration of protein in each fraction was determined by spectrophotometry measuring absorbance at 280 nm (Fig. S1). The column was washed with the starting buffer until reaching a minimum of protein concentration. The α-amylase was recovered from the column with 40 mM acetate buffer (pH 5.2) containing 10 $mgmL^{-1}$ maltose. Enzyme activities in fractions were ascertained by spectrophotometry at 400 nm applying the appropriate chromogenic substrates: PNP-α- and β-D-glucopyranoside (Sigma-Aldrich, St. Louis, Missouri, USA) and 2-chloro-4-nitrophenyl O-β-D-galactopyranosyl-(1 → 4)-O-α-D-glucopyranosyl-(1 → 4)-α-D-glucopyranoside (GalG2CNP Fig. 1A, SORACHIM S.A., Lausanne, Switzerland) for α- and β-glucosidase and α-amylase, respectively. (Data of amylase activity measurements are presented in the Supplementary material as Fig. S1) Fractions showing α-amylase activity were combined then concentrated and washed with 50 mM 2-(N-morpholino)-ethanesulfonic acid (MES) buffer pH 6.0 containing 5 mM $Ca(OAc)_2$ and 51.5 mM NaCl using 30 K centrifugal filter unit (Merck, Darmstadt, Germany) at 7000*g*. Neither α- nor β-glucosidase activity was detected in fractions 28–40.

2.2. Homogeneity of LdAmy

Purified LdAmy was analyzed using denaturing sodium dodecylsulfate-polyacrylamide gel electrophoresis (SDS-PAGE). Discontinuous polyacrylamide gel as a support medium consisted of 5% stacking and 8% separation gel, and separation was performed as described by Laemmli [32]. Molecular weight markers were obtained from ProSieve QuadColor™ protein marker (molecular weight range 4.6 kDa–300 kDa, purchased from Lonza). Running buffer of the denaturing electrophoresis was 250 mM Tris-glycine buffer, pH 8.3, containing 1% SDS. The electrophoresis was carried out in MINI-PROTEAN II electrophoretic unit (BIO-RAD). Protein bands were stained with 0.25% w/v Coomassie blue R-250. The SDS-PAGE gel image (Fig. S2) verify the homogeneity of LdAmy and resulted in ~55 kDa molecular weight for the purified protein.

2.3. Measurement of enzyme activities

Kinetic experiments were carried out at 30 °C in 50 mM MES (Sigma-Aldrich, St. Louis, Missouri, USA) buffer pH 6.0 containing 5 mM $Ca(OAc)_2$ (Reanal, Budapest, Hungary), 51.5 mM NaCl (MOLAR, Budapest, Hungary), and 152 mM NaN_3 (Sigma-Aldrich, St. Louis, Missouri, USA) using $GalG_2CNP$ as α-amylase substrate. This buffer composition is optimal for exclusive aglycone cleavage by α-amylases [33]. A 200 μL aliquots of 5 mM substrate and MES buffer of 290 μL were mixed in a half-micro cuvette and incubated at 37 °C for 5 min. The reaction was initiated by adding a 10 μL aliquot of enzyme solution and continuous measurement of absorbance started immediately. Kinetic curves of CNP (2-chloro-4-nitrophenyl) release were measured continuously at 400 nm using the Parallel Kinetics Analysis program of a JASCO V550 spectrophotometer (Jasco Corporation, Easton, MD,

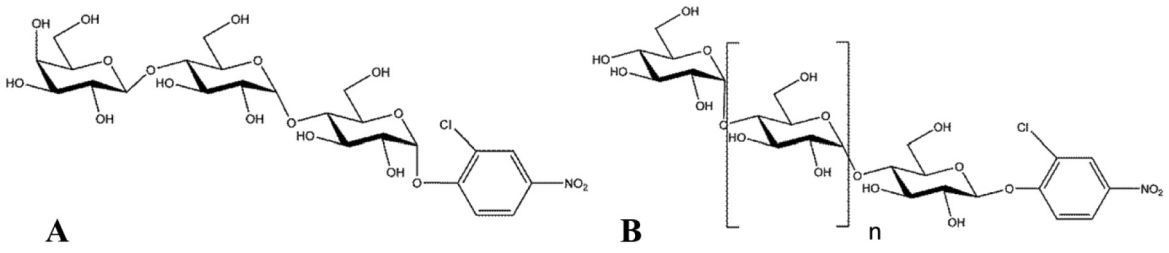

Fig. 1. Structure of α-amylase substrates. A) 2-Chloro-4-nitrophenyl 4-O-β-D-galactopyranosyl-α-maltoside; B) 2-Chloro-4-nitrophenyl β-maltooligomers ($CNPG_n$; n = 4–8).

USA). Progress curves were fitted using linear regression. All experiments were repeated three or five times. Normalized ΔA min^{-1} values, proportional to initial rate, were considered to be enzyme activities.

2.4. HPLC action pattern determination

Hydrolysis reaction in 1 mL solution of a 2-chloro-4-nitrophenyl β-maltooligomer (100 μM) substrate ($CNPG_n$, Fig. 1B) was initiated by the addition of 5 μL purified LdAmy, and 5 μL samples were repeatedly injected in every 20 min. Agilent 1260 Infinity II (Quaternary pump, Vial sampler, Diode Array Detector) liquid chromatograph and a Venusil AQ C18 column (4.6 × 150 mm, 3 μm, Agela) were used for each separation. Isocratic elution was used for the separation of products applying an eluent containing 18% (V/V) acetonitrile in water with a flow rate of 0.6 mL min^{-1}. HPLC grade acetonitrile (VWR, France) and purified water from a MilliQ system with ion-exchange and carbon filter (Millipore, Bedford, MA, USA) were used for eluent. The temperature of the column and vial sampler was maintained at 40 °C. Compounds bearing chromophore aglycone were detected by a diode array detector at 302 nm (see a sample chromatogram as Fig. S3 in Supplementary file). BCF values were calculated by dividing the peak area of each product with the sum of the product areas. Peak areas obtained for individual oligosaccharides were converted into molar concentrations, which were plotted as a function of reaction time to obtain the progress curves.

2.5. Data evaluation by Scientist® program

Concentration-time data pairs were transported into the Scientist® program (Micromath St. Luis, USA). Kinetic constants (k) were determined assuming parallel reactions as first hydrolysis steps followed by consecutive reactions. A kinetic model of LdAmy-catalysed hydrolysis was developed. (A scheme of parallel and consecutive steps is presented in Supplementary material for the octamer reaction as an example, see Fig. S4). The octamer substrate molecule (S_8) was hydrolysed by LdAmy with parallel reactions into tetramer (S_4), trimer (S_3) and dimer (S_2) chromophore labelled products. The apparent rate constants of parallel steps are k_{nx}, where n is the number of monomer unit (G-glucose) in the substrate, x is the number of G unit in the reducing-end product. Further consecutive hydrolysis steps can occur on the reaction products catalysed by the same enzyme, producing S_3, S_2 and S from tetramer as well as S from trimer.

Differential equations (Eqns 1, 2, 3, 4 and 5) can be written for the temporal variations of the concentrations of the substrates and the final products:

$$\frac{d[S_8]}{dt} = -k_{84}[S_8] - k_{83}[S_8] - k_{82}[S_8] \quad (1)$$

$$\frac{d[S_4]}{dt} = k_{84}[S_8] - k_{43}[S_4] - k_{42}[S_4] - k_{41}[S_4] \quad (2)$$

$$\frac{d[S_3]}{dt} = k_{83}[S_8] + k_{43}[S_4] - k_{31}[S_3] \quad (3)$$

$$\frac{d[S_2]}{dt} = k_{82}[S_8] + k_{42}[S_4] \quad (4)$$

$$\frac{d[S]}{dt} = k_{41}[S_4] + k_{31}[S_3] \quad (5)$$

2.6. Subsite map calculation

Detailed description of SUMA program used for subsite map calculations had been published earlier [30]. The software calculates the apparent binding energies on the basis of the measured bond cleavage frequencies. Briefly, the calculations are based on the following equation (Eqn 6):

$$\Delta G_{\iota+1} + \Delta G_{\chi} = -RT * \ln \frac{P_{\iota}}{P_{\iota+1}} \quad (6)$$

where $\Delta G_{\iota+1}$ is the subsite binding energy of the subsite $\iota + 1$, ΔG_X is the subsite binding energy of the subsite x, P_ι and $P_{\iota+1}$ are the bond cleavage frequencies of the products which are produced from the binding mode, in which the reducing end of the substrate is connected to the subsites ι and ι + 1, respectively. The number of subsites and the position of the cleavage site can be set arbitrary for the calculations. The primary calculated subsite energy values can be refined until reaching the best agreement of the measured and recalculated BCF data by an iteration process.

3. Results and discussion

3.1. Action pattern and cleavage frequencies of LdAmy on CNP-maltooligosaccharides

A series of $CNPG_n$ (n = 4–8) maltooligomers was hydrolyzed by LdAmy and followed by HPLC in order to determine the exact position of glycosidic linkage being cleaved as well as the cleavage frequencies that indicate the binding mode of the corresponding substrate. Only the chromogenic reaction products formed were quantified, and the results are given in Table 1. as an average of at least three determinations.

LdAmy exhibits a unique pattern of action on CNP-maltooligosaccharides by cleaving $CNPG_2$ reducing end product from $CNPG_4$, $CNPG_5$ and $CNPG_6$ with the ratios of 0.47, 1.00 and 0.70 and accordingly maltose, maltotriose and maltotetraose are also released as non-reducing end products. As the chain length increases, the maximum frequency of attack shifts toward the non-reducing end of the substrate. In case of $CNPG_7$ and $CNPG_8$, a more equal distribution can be observed in the product ratios, but the release of maltotetraose is always dominant. It is important to note that the ratios of $CNPG_3$ and $CNPG_4$ products are almost equal at the beginning of the hydrolysis of the heptamer substrate. $CNPG_3$ is also present as a product of hydrolysis even in case of the shortest tetramer substrate. Our results are in good agreement with the previous ones obtained for the heptamer substrate [26] which suggest a semblance between the subsite structure of LdAmy and that of PPA.

3.2. Hydrolysis of individual substrates by LdAmy

The prolonged hydrolysis of chromophore containing oligomer substrates were followed by HPLC. The obtained data and fitted progress curves are presented in Fig. 2. Data evaluation was carried out by analyzing the progress curves for each hydrolysis reaction using reaction schemes containing parallel and consecutive steps. In this case, the mathematical model is a complex system of differential equations obtained from the assumed reaction scheme (Fig. S4). Scientist® software allows numerical solution of differential equations.

Table 1
BCFs from the hydrolysis of maltooligomer substrates by LDAmy.

Substrate	2-Chloro-4-nitrophenyl glycoside products (mol/mol)			
	CNPG	$CNPG_2$	$CNPG_3$	$CNPG_4$
$CNPG_4$	0.34	0.47	0.19	
$CNPG_5$		1.00		
$CNPG_6$		0.70	0.30	
$CNPG_7$		0.39	0.40	0.21
$CNPG_8$		0.30	0.30	0.39

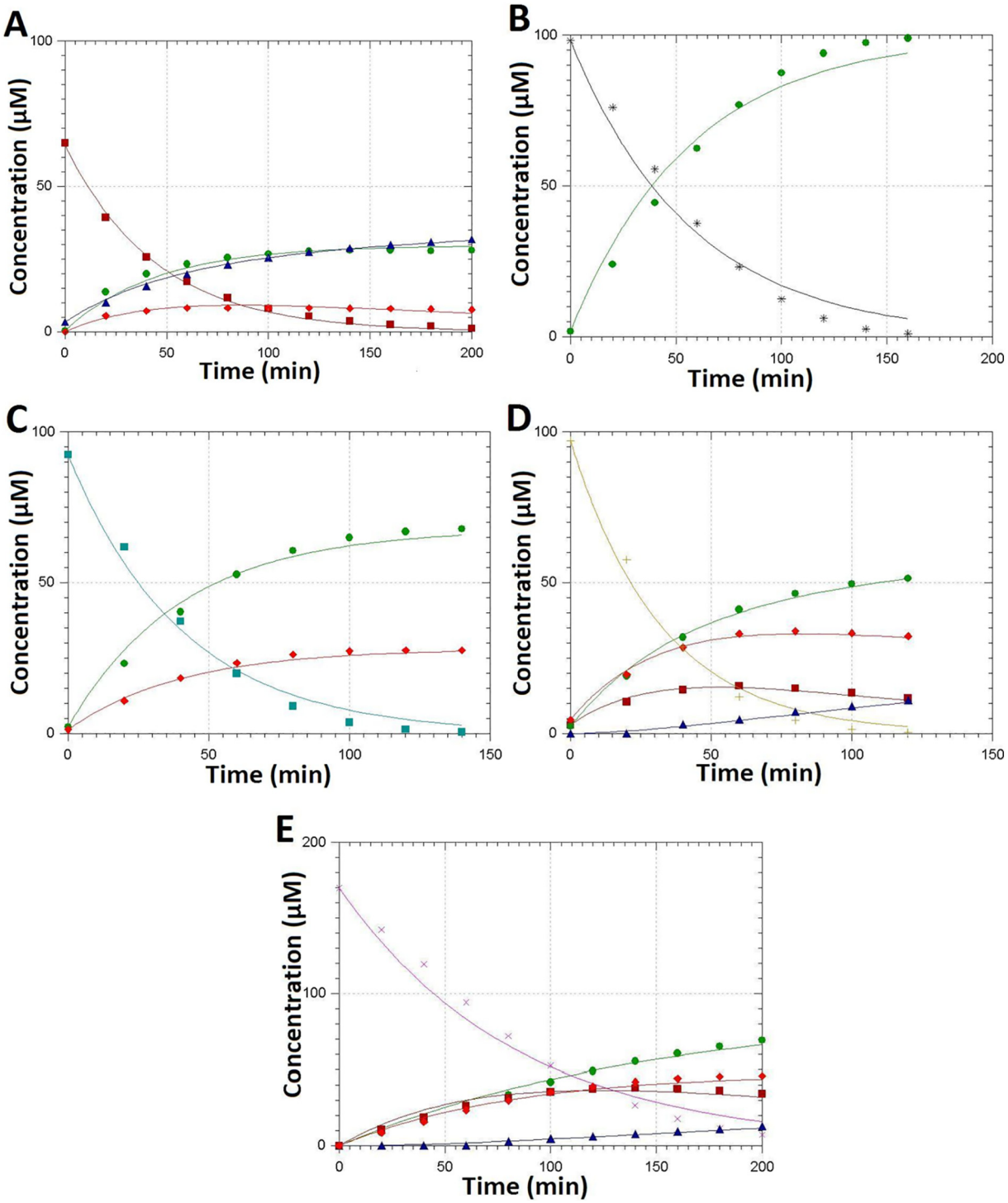

Fig. 2. Progress curves of hydrolysis reactions catalysed by LdAmy on 100 μM CNP-maltooligomers in MES buffer pH 6.8. Substrate and product conentrations were calculated from peak area of compounds after separation by HPLC. Substrates were as follows: A) $CNPG_4$ red ■; B) $CNPG_5$ *; C) $CNPG_6$ turquoise ■; D) $CNPG_7$ green +; E) $CNPG_8$ lilac ×. Products of hydrolysis CNPG blue; $CNPG_2$ green ●; $CNPG_3$ red ◊.

Enzymatic hydrolysis of $CNPG_5$ was considered as a simple one-step process since the primer product ($CNPG_2$) is not a substrate for α-amylases (Fig. 2B). Curves were fitted using a simple one-step model. Calculated kinetic constants for the investigated five substrates are summarized in Table 2. The hydrolysis of the substrates except $CNPG_5$ resulted in more products as a consequence of parallel reaction steps due to the different binding modes of substrates. Consecutive steps were assumed for $CNPG_7$ and $CNPG_8$ substrates (Fig. 2D and E), which were long enough to result in the formation of further hydrolysable primary reducing-end products (tetramer and trimer).

The ratios of obtained kinetic constants for the first parallel steps are in good agreement with the bond cleavage frequency data (Fig. S5) showing that our hypothesized model describes the process of hydrolysis in an appropriate manner. Calculated kinetic constants for secondary hydrolysis of $CNPG_4$ product and for primary hydrolysis of $CNPG_4$ substrate differed from each other, but the symmetrical cleavage (resulted

Table 2
Kinetic constants for LdAmy catalysed hydrolysis reactions of CNP-β-G_n oligomer substrates (n = 4–8).

Parameter	Kinetic constants (10^3 min^{-1}) for substrates				
	$CNPG_8$	$CNPG_7$	$CNPG_6$	$CNPG_5$	$CNPG_4$
k_{84}	4.90				
k_{83}	3.42				
k_{82}	3.56				
k_{74}		7.17			
k_{73}		11.92			
k_{72}		12.0			
k_{63}			7.37		
k_{62}			17.32		
k_{52}				17.5	
k_{43}	0.706	1.0			4.93
k_{42}	3.428	8.07			10.22
k_{41}	1.193	0.76			7.23
k_{31}	0.757	2.74			5.04

in dimer products from reducing and nonreducing end) was preferred similarly in all cases.

3.3. Calculation of subsite map: evidence for a "six-subsite" model

Data of Table 1 were used for subsite map calculations by SUMA software. The apparent free energy values were optimized by minimization of the differences of the measured and calculated BCF data.

Our results strongly suggest the presence of at least six subsites, four glycone- and two aglycone-binding sites, in the binding region of LdAmy similarly to the subsite structure of PPA determined earlier [30]. Fig. 3 shows the subsite maps and the apparent binding energies of subsites for HSA, LdAmy and PPA. The subsites are labelled, according to the nomenclature proposed by Davies et al. [34], with negative numbers to the left (non-reducing end site) and positive numbers to the right (reducing end site) from the cleavage site. A '4 + 2 model' is suggested for LdAmy, where the interaction between the glucose unit and subsite is favorable at subsites (−3) and (+2) whereas less favorable at subsites (−2) and (−4). However, a very interesting, unique phenomenon can be observed at the glycone binding site in the energy levels. In contrast to the tendencies of both HSA and PPA, where a continuous decrease is observed moving away from the catalytic site, in the case of LDAmy the energy of subsite (−3) is the largest. To interpret the

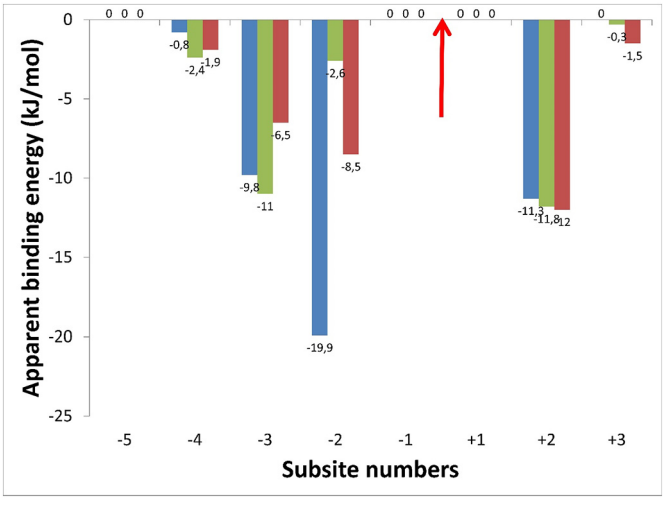

Fig. 3. Subsite maps of LdAmy (green) HSA (blue) and PPA (red). The subsites are labelled with negative numbers to the left (glycone binding site) and positive numbers to the right (aglycone binding site) from the cleavage site, the arrow indicates the location of hydrolysis.

observed differences, we compared amino acid sequence of alpha-amylase like protein of L. decemlineata to that of known α-amylases such as HSA, PPA, and Tenebrio molitor α-amylase. Multiple sequence alignment was made using CLUSTAL Omega version 1.2.4 (see in Supplement as Fig. S5.) Amino acids involving in substrate binding were summarized in Table 3.

Sequence identities are low between these proteins, but similarity is far better especially in conserved regions. Catalytic amino acids (Asp197 and Glu233) and amino acid residues at the aglycone binding sites (+1) and (+2) are identical, but there are some notable differences at the glycone binding region (Table 3). In LdAmy, subsite (−4) contains a polar but uncharged amino acid (Thr) at position 147, where a non-polar one (Gly) can be found in PPA. However, two acidic amino acids (Asp) and (Glu) are at the same position of HSA and TMA. These differences may justify the slight difference that appears on the subsite map at this position. There is a much larger difference in the binding energy and polarity of the amino acids surrounding subsite (−2).

Positively charged amino acid (His305) present in HSA and PPA is replaced by an acidic, negatively charged (Asp) in LdAmy and by an apolar Gly in TMA. In addition, His101 near this subsite is also changed to Asp in case of LdAmy. Interestingly, an apolar amino acid Val163 can be found at subsite (−3) in all of the studied enzyme except HSA.

4. Conclusions

Considering our findings, we think that LdAmy was an interesting enzyme for *in vitro* and *in silico* studies. The use of modified, low molecular weight substrates allowed to elucidate the action pattern and product specificity of LdAmy, which have not been examined so far and just as sub-site map has not been available for any insect. We have presented the first subsite map for an insect α-amylase and our results have revealed that the binding region in LdAmy is similar to mammalian α-amylases HSA and PPA and suggested the presence of six subsites. However, we observed differences in energy levels at the glycone binding sites. Multiple sequence alignment revealed that the variation in polarity of amino acids present in the glycone binding site is responsible for the differences. It became clear that there are also sequence differences between LdAmy and TMA, and the later had greater sequence similarity to HSA and PPA at the active site.

Table 3
Amino acid residues involved in substrate binding of different α-amylases.

Subsite	Amino acid[a] (and position in HSA)			
	HSA[b]	LdAmy	PPA	TMA
-4	Asp147	**Thr147**	**Gly147**	Glu147
	Asn105	Gln105	**Ser105**[c]	**Met105**
-3	**Ser163**	Val163	Val163	Val163
	Gln63	Gln63	Gln63	Gln63
	Asp356	Asp356	Asp356	Asp356
-2	Trp58	Trp58	Trp58	Trp58
	Trp59	Trp59	Trp59	Trp59
	Tyr62	Tyr62	Tyr62	Tyr62
	His305	**Asp305**	His305	**Gly305**
-1	His101	**Asp101**	His101	His101
	Arg195	Arg195	Arg195	Arg195
	Asp197	*Asp197*	*Asp197*	*Asp197*
	His299	His299	His299	His299
	Asp300	Asp300	Asp300	Asp300
+1	His201	His201	His201	His201
	Glu233	*Glu233*	*Glu233*	*Glu233*
	Ile235	Ile235	Ile235	Ile235
+2	Tyr151	Tyr151	Tyr151	Tyr151
	Lys200	Lys200	Lys200	Lys200
	Glu240	Glu240	Glu240	Glu240

Bold characters indicate differences.
[a] Amino acid numbering corresponds to the 1SMD HSA sequence.
[b] Active site position in HSA [35].
[c] Active site position in PPA [36].

CRediT authorship contribution statement

Csaba Hámori: Methodology, Investigation, Formal analysis, **Judit Remenyik:** Resources, Methodology, **Lili Kandra:** Supervision, Writing - review & editing, **Gyöngyi Gyémánt:** Conceptualization, Writing - original draft, Visualization, Writing - review & editing.

Declaration of competing interest

None.

Acknowledgements

The research was supported by the EU and co-financed by the European Regional Development Fund under the project GINOP-2.3.2-15-2016-00008.

Appendix A. Supplementary data

Supplementary data to this article can be found online at https://doi.org/10.1016/j.ijbiomac.2020.12.071.

References

[1] W.R. Terra, C. Ferreira, Biochemistry and molecular biology of digestion, in: L. Gilbert (Ed.), Insect Molecular Biology and Biochemistry, Academic Press, Cambridge, Massachusetts, USA 2012, pp. 366–418.
[2] P.H. Boer, D.A. Hickey, The alpha-amylase gene in *Drosophila melanogaster*: nucleotide sequence, gene structure and expression motifs, Nucleic Acids Res. 14 (1986) 8399–8411.
[3] R. Charlab, J.G. Valenzuela, E.D. Rowton, J.M. Ribeiro, Toward an understanding of the biochemical and pharmacological complexity of the saliva of a hematophagous sand fly, *Lutzomyia longipalpis*, Proc. Natl. Acad. Sci. U. S. A. 96 (1999) 15155–15160.
[4] K. Ohashi, S. Natori, T. Kubo, Expression of amylase and glucose oxidase in the hypopharyngeal gland with an age-dependent role change of the worker honeybee *(Apis mellifera L.)*, Eur. J. Biochem. 265 (1999) 127–133.
[5] M.S. Khorram, R.F.P. Abad, M. Yazdaniyan, S. Jafarnia, Digestive alpha-amylase from *Leptinotarsa decemlineata* (Say) (Coleoptera: Chrysomelidae); response to pH, temperature and some mineral compounds, Adv. Environ. Biol. 4 (2010) 101–107.
[6] E. Titarenko, M.J. Chrispeels, cDNA cloning, biochemical characterization and inhibition by plant inhibitors of the α-amylases of the Western corn rootworm, *Diabrotica virgifera virgifera*, Insect Biochem. Mol. Biol. 30 (2000) 979–990, https://doi.org/10.1016/j.jinsphys.2010.02.020.
[7] F. Zeng, A.C. Cohen, Partial characterization of alpha-amylase in the salivary glands of *Lygus hesperus* and *L. lineolaris*, Comp. Biochem. Physiol. B Biochem. Mol. Biol. 126 (2000) 9–16.
[8] M.F. Grossi de SaÂ, M.J. Chrispeels, Molecular cloning of bruchid (*Zabrotes subfasciatus*) α-amylase cDNA and interactions of the expressed enzyme with bean amylase inhibitors, Insect Biochem. Mol. Biol. 27 (1997) 271–281.
[9] V. Buonocore, E. Poerio, V. Silano, M. Tomasi, Physical and catalytic properties of α-amylase from *Tenebrio molitor* L. larvae, Biochem. J. 153 (1976) 621–625.
[10] V. Nahoum, F. Farisei, V. Le-Berre-Anton, M.P. Egloff, P. Rougé, E. Poerio, F. Payan, A plant-seed inhibitor of two classes of α-amylases: X-ray analysis of *Tenebrio molitor* larvae α-amylase in complex with the bean *Phaseolus vulgaris* inhibitor, Acta Cryst D55 (1999) 360–362.
[11] V. Lombard, H. Golaconda Ramulu, E. Drula, P.M. Coutinho, B. Henrissat, The carbohydrate-active enzymes database (CAZy) in 2013, Nucleic Acids Res. 42 (D) (2014) 490–D495.
[12] S. Janecek, Alpha-amylase family: molecular biology and evolution, Prog. Biophys. Mol. Biol. 67 (1997) 67–97, https://doi.org/10.1016/s0079-6107(97)00015-1.
[13] D. Philips, The three-dimensional structure of an enzyme molecule, Sci. Am. 215 (1966) 78–90.
[14] J.D. Allen, J.A. Thoma, Subsite mapping of enzymes. Depolymerase computer modeling, Biochem. J. 159 (1976) 105–120.
[15] J.D. Allen, J.A. Thoma, Subsite mapping of enzymes. Application of depolymerase computer model to two α-amylases, Biochem. J. 159 (1976) 121–132.
[16] L. Kandra, G. Gyémánt, E. Farkas, A. Lipták, Action pattern of porcine pancreatic alpha-amylase on three different series of β-maltooligosaccharide glycosides, Carbohydr. Res. 298 (1997) 237–242.
[17] L. Kandra, G. Gyémánt, J. Remenyik, G. Hovánszki, A. Lipták, Action pattern and subsite mapping of *Bacillus licheniformis* α-amylase (BLA) with modified maltooligosaccharide substrates, FEBS Lett. 518 (2002) 79–82.
[18] L. Kandra, G. Gyémánt, J. Remenyik, C. Ragunath, N. Ramasubbu, Subsite mapping of human salivary α-amylase and the mutant Y151M, FEBS Lett. 544 (2003) 194–198.
[19] L. Kandra, M.A. Hachem, G. Gyémánt, B. Kramhøft, B. Svensson, Mapping of barley α-amylases and outer subsite mutants reveals dynamic high-affinity subsites and barriers in the long substrate binding cleft, FEBS Lett. 580 (2006) 5049–5053.
[20] R. Jbilou, H. Amri, N. Bouayad, N. Ghailani, A. Ennabili, F. Sayah, Insecticidal effects of extracts of seven plant species on larval development, alpha-amylase activity and offspring production of *Tribolium castaneum* (Herbst) (Insecta: Coleoptera: Tenebrionidae), Bioresour. Technol. 99 (2008) 959–964, https://doi.org/10.1016/j.biortech.2007.03.017.
[21] K.V.G. Lopes, L.B. Silva, A.P. Reis, R.N.C. Oliveira, M.G.A. Guedes, Modified alpha-amylase activity among insecticide-resistant and -susceptible strains of the maize weevil, *Sitophilus zeamais*, J. Insect Physiol. 56 (2010) 1050–1057.
[22] A. Valencia-Jiménez, J.W. Arboleda, A.L. Avila, M.F. Grossi-de-Sá, Digestive alpha-amylases from *Tecia solanivora* larvae (*Lepidoptera: Gelechiidae*). Response to pH, temperature and plant amylase inhibitors, Bull. Entomol. Res. 98 (6) (2008) 575–579, https://doi.org/10.1017/S0007485308005944.
[23] S.M. Channale, A.J. Bhide, Y. Yadav, G. Kashyap, P.K. Pawar, V.L. Maheshwari, S. Ramasamy, A.P. Giri, Characterization of two coleopteran α-amylases and molecular insights into their differential inhibition by synthetic α-amylase inhibitor, acarbose, Insect Biochem. Mol. Biol. 74 (2016) 1–11.
[24] P.B. Pelegrini, A.M. Murad, M.F. Grossi-de-Sá, L.V. Mello, L.A.S. Romeiro, E.F. Noronha, R.A. Caldas, O.L. Franco, Structure and enzyme properties of *Zabrotes subfasciatus* alpha-amylase, Arch. Insect Biochem. Physiol. 61 (2006) 77–86, https://doi.org/10.1002/arch.20099.
[25] K.D. Saltzmann, K.A. Saltzmann, J.J. Neal, M.E. Scharf, G.W. Bennett, Characterization of BGTG-1, a tergal gland-secreted alpha-amylase, from the German cockroach, *Blattella germanica* (L.), Insect Mol. Biol. 15 (2006) 425–433.
[26] E. Szilágyi, C. Hámori, P. Bíró-Molnár, L. Kandra, J. Remenyik, G. Gyémánt, Cooperation of enzymes involved in carbohydrate digestion of Colorado potato beetle (*Leptinotarsa decemlineata*, Say), Bull. Entomol. Res. 109 (2019) 695–700, https://doi.org/10.1017/S0007485319000099.
[27] S.D. Schoville, Y.H. Chen, M.N. Andersson, J.B. Benoit, A. Bhandari, J.H. Bowsher, K. Brevik, K. Cappelle, M.M. Chen, A.K. Childers, C. Childers, O. Christiaens, J. Clements, E.M. Didion, E.N. Elpidina, P. Engsontia, M. Friedrich, I. García-Robles, R.A. Gibbs, C. Goswami, A. Grapputo, K. Gruden, M. Grynberg, B. Henrissat, E.C. Jennings, J.W. Jones M. Kalsi, S.A. Khan, A. Kumar, F. Li, V. Lombard X. Ma, A. Martynov, N.J. Miller, R.F. Mitchell, M. Munoz-Torres, A. Muszewska, B.S.R. OppertPalli, K.A.Y. Panfilio, L.C. Perkin Pauchet, M. Petek, M.F. Poelchau, J.P. Record, J.P. Rinehart, H.M. Robertson, A.J. Rosendale, V.M. Ruiz-Arroyo, G. Smagghe, Z. Szendrei, G.W.C. Thomas, A.S. Torson, I.M.V. Jentzsch, M.T. Weirauch, A.D. Yates, G.D. Yocum, J. Yoon, S. Richards, A model species for agricultural pest genomics: the genome of the Colorado potato beetle, *Leptinotarsa decemlineata* (Coleoptera: Chrysomelidae), Sci. Rep. 8 (2018) 1931, https://doi.org/10.1038/s41598-018-20154-1.
[28] M. Nawaz, M. Taha, F. Qureshi, N. Ullah, M. Selvaraj, S. Shahzad, S. Chigurupati, A. Waheed, F.A. Almutairi, Structural elucidation, molecular docking, α-amylase and α-glucosidase inhibition studies of 5-amino-nicotinic acid derivatives, BMC Chemistry 14 (2020), 43, https://doi.org/10.1186/s13065-020-00695-1.
[29] I. Ali, R. Rafique, K.M. Khan, S. Chigurupati, X. Ji, A. Wadood, A.U. Rehman, U. Salar, M.S. Iqbal, M. Taha, S. Perveen, B. Ali, Potent α-amylase inhibitors and radical (DPPH and ABTS) scavengers based on benzofuran-2-yl(phenyl)methanone derivatives: syntheses, in vitro, kinetics, and in silico studies, Bioorg. Chem. 104 (2020), 104238, https://doi.org/10.1016/j.bioorg.2020.104238.
[30] G. Gyémánt, G. Hovánszki, L. Kandra, Subsite mapping of the binding region of α-amylases with a computer program, Eur. J. Biochem. 26 (9) (2002) 5157–5162.
[31] M. Kobayashi, Y. Sasaki, S. Kobayashi, Purification of amylases and other enzymes by a forced-affinity chromatography method, Biosci. Biotechnol. Biochem. 61 (5) (1997) 813–5816, https://doi.org/10.1271/bbb.61.813U.K.
[32] Laemmli, Cleavage of structural proteins during the assembly of the head of bacteriophage T4, Nature 227 (1970) 680–685.
[33] Y. Morishita, Y. Iinuma, N. Nakashima, K. Majima, K. Mizuguchi, Y. Kawamura, Total and pancreatic amylase measured with 2-chloro-4-nitrophenyl 4-O-β-D-galactopyranosylmaltoside, Clin. Chem. 46 (2000) 928–933.
[34] G.J. Davies, K.S. Wilson, B. Henrissat, Nomenclature for sugar-binding subsites in glycosyl hydrolases, Biochem. J. 321 (1997) 557–559.
[35] N. Ramasubbu, V. Paloth, Y. Luo, G.D. Brayer, M.J. Levine, Structure of human salivary alpha-amylase at 1.6 a resolution: implications for its role in the oral cavity, Acta Crystallogr. D. Biol. Crystallogr. 52 (Pt 3) (1996) https://doi.org/10.1107/S0907444995014119 1. 435-46.
[36] C. Gilles, J.P. Astier, G. Marchis-Mouren, C. Cambillau, F. Payan, Crystal structure of pig pancreatic alpha-amylase isoenzyme II, in complex with the carbohydrate inhibitor acarbose, Eur. J. Biochem. 238 (1996) 561–569, https://doi.org/10.1111/j.1432-1033.1996.0561z.x.